Chemical Science

Accepted Manuscript

Chemical Science

rsc.li/chemical-science

Volume 9
Number 1
7 January 2018
Pages 1-268

ISSN 2041-6539

ROYAL SOCIETY OF CHEMISTRY

EDGE ARTICLE
Xinjing Tang et al.
Caged circular siRNAs for photomodulation of gene expression in cells and mice

This is an Accepted Manuscript, which has been through the Royal Society of Chemistry peer review process and has been accepted for publication.

Accepted Manuscripts are published online shortly after acceptance, before technical editing, formatting and proof reading. Using this free service, authors can make their results available to the community, in citable form, before we publish the edited article. We will replace this Accepted Manuscript with the edited and formatted Advance Article as soon as it is available.

You can find more information about Accepted Manuscripts in the Information for Authors.

Please note that technical editing may introduce minor changes to the text and/or graphics, which may alter content. The journal's standard Terms & Conditions and the Ethical guidelines still apply. In no event shall the Royal Society of Chemistry be held responsible for any errors or omissions in this Accepted Manuscript or any consequences arising from the use of any information it contains.

ROYAL SOCIETY OF CHEMISTRY

rsc.li/chemical-science

ARTICLE

Access to Allyl-*gem*-difluorides via Allylation and Cope Rearrangement

Haeun Kim,[a,+] Seungcheol Han,[a,+] Yunhui Jang,[a] Yujin Jung[a] and Seung Hwan Cho[a,*]
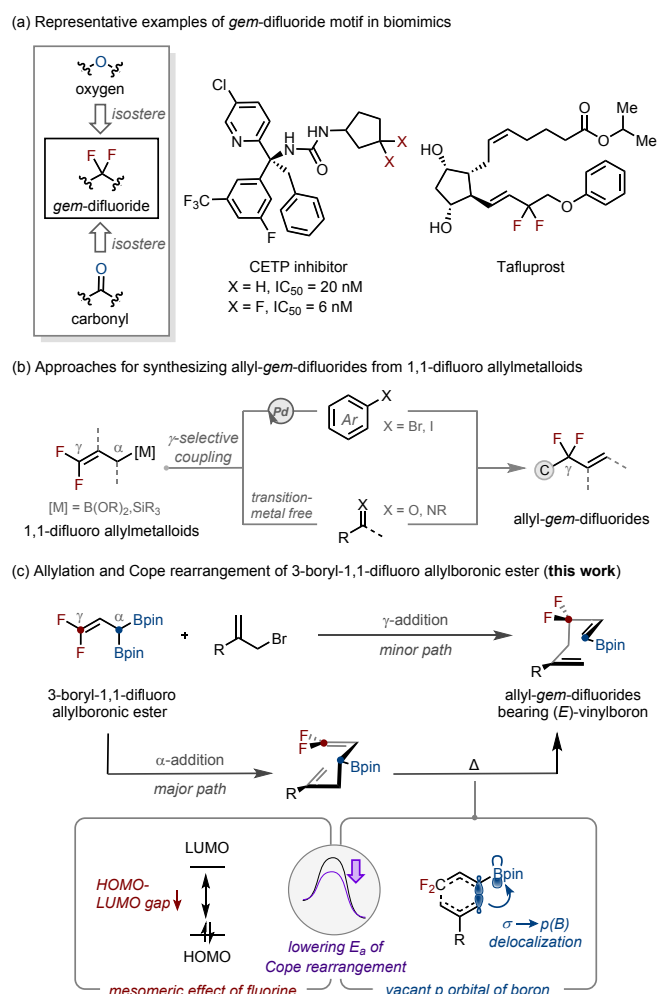
Fluorinated molecules play crucial roles in medicinal and materials chemistry, as the presence of fluorine profoundly alters molecular electronics and reactivity. Among them, allyl *gem*-difluorides have attracted growing attention as versatile synthetic intermediates, but their selective construction remain challenging. Here, we disclose an efficient strategy for synthesizing allyl *gem*-difluorides bearing (*E*)-vinyl boronic esters through a LiO*t*Bu-mediated deborylative allylation/Cope rearrangement sequence of 3-boryl-1,1-difluoro allylboronic ester with allyl bromides. Four competing pathways (α-S_N2, α-S_N2', γ-S_N2, and γ-S_N2') were identified: α-addition generates intermediates that undergo Cope rearrangement, while γ-addition directly delivers the same products. Mechanistic studies, supported by control experiments as well as NBO and FMO analyses, demonstrate a synergistic effect between the 1,1-difluoro group and the boronic ester that lowers the activation barrier of the rearrangement. This transformation displays broad substrate scope and provides versatile building blocks for the construction of allyl *gem*-difluorides.

Introduction

Fluorine-containing organic molecules play pivotal roles in agrochemicals, pharmaceuticals, and advanced materials owing to their distinctive physicochemical properties.[1] Among fluorinated motifs, the difluoromethylene (CF_2) unit serves as a valuable bioisostere of oxygen and carbonyl groups, imparting unique features such as altered dipole moments, increased acidity of adjacent bonds, and characteristic conformational preferences (Scheme 1a).[2] These attributes often translate into enhanced metabolic stability and biocompatibility in drug-like molecules.[3] Within this context, allyl *gem*-difluorides represent a particularly intriguing class of molecules because of their unique chemical reactivity and potential applications in the design of bioactive compounds.[4,5]

Over the past decades, various approaches have been developed for the synthesis of allyl *gem*-difluorides.[6,7] Among these, 1,1-difluoro allylmetalloids have proven to be versatile building blocks for the incorporation of a difluoromethylene unit (Scheme 1b). These reagents have enabled Pd-catalyzed *gem*-difluoroallylation of aryl halides[8] as well as transition-metal free allylation of carbonyls and imines,[9] thereby providing efficient access to allyl *gem*-difluorides. Nevertheless, the use of 1,1-difluoro allylmetalloids has so far been applied primarily to the synthesis of allyl *gem*-difluorides bearing terminal alkenes. Transformations affording allyl *gem*-difluorides bearing a 1,2-disubstituted internal alkene unit are rare[9f,9m] and often proceed with poor E/Z selectivity.[8b,9b] Therefore, the development of a new 1,1-difluoro allylmetalloid reagent and a

(a) Representative examples of *gem*-difluoride motif in biomimics

CETP inhibitor
X = H, IC_{50} = 20 nM
X = F, IC_{50} = 6 nM

Tafluprost

(b) Approaches for synthesizing allyl-*gem*-difluorides from 1,1-difluoro allylmetalloids

[M] = B(OR)$_2$,SiR$_3$
1,1-difluoro allylmetalloids

γ-selective coupling

transition-metal free

X = Br, I

X = O, NR

allyl-*gem*-difluorides

(c) Allylation and Cope rearrangement of 3-boryl-1,1-difluoro allylboronic ester (**this work**)

3-boryl-1,1-difluoro allylboronic ester

γ-addition
minor path

α-addition
major path

Δ

allyl-*gem*-difluorides bearing (*E*)-vinylboron

LUMO

HOMO

HOMO-LUMO gap ↓

lowering E_a of Cope rearrangement

mesomeric effect of fluorine

$\sigma \rightarrow p(B)$ delocalization

vacant p orbital of boron

Scheme 1 Approaches for synthesizing allyl *gem*-difluoride. Bpin: (pinacolato)boryl.

[a.] *Department of Chemistry, Pohang University of Science and Technology (POSTECH), Pohang, 37673, Rep. of Korea. E-mail: seunghwan@postech.ac.kr*
Electronic Supplementary Information (ESI) available: See DOI: 10.1039/x0xx00000x

(a) Synthesis of 3-boryl-1,1-difluoro allylboronic ester
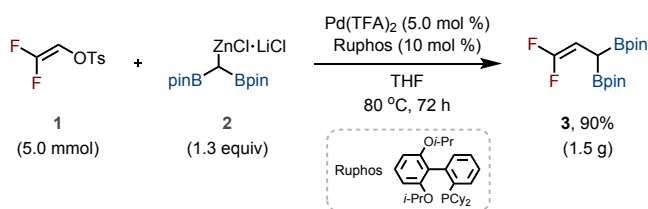
(b) Evaluation of reaction conditions^a
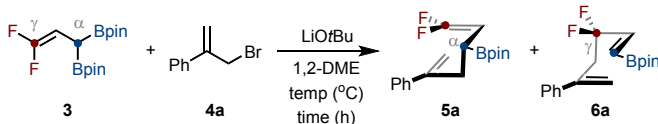
entry	temp (^{o}C)	time	yield (%)^b	
			5a	**6a**
1	80	1 h	59	25
2	80	12 h	26	56
3	80	24 h	-	88
4	50	24 h	49	21
5	rt	24 h	55	19
6	0	24 h	62	20

(c) Control experiments

(d) Deuterium-labeling experiments

Scheme 2 Reaction discovery. ^{a}**4a** (0.1 mmol), **3** (0.22 mmol), LiOtBu (0.22 mmol), 1,2-DME (0.20 M) at indicated temperature and time. The ^{1}H NMR yield was determined using CH$_2$Br$_2$ as an internal standard. TFA: trifluoroacetate; i-Pr: isopropyl; Cy: cyclohexyl; THF: tetrahydrofuran; 1,2-DME: 1,2-dimethoxyethane; Ph: phenyl.

complementary synthetic platform capable of delivering allyl *gem*-difluorides bearing 1,2-disubstituted internal alkenes with high stereocontrol remains a significant challenge.

As part of our ongoing research on *gem*-diboron chemistry,[10] we envisioned that incorporating fluorinated motifs into *gem*-diboryl frameworks[11] would provide an effective platform for accessing fluorine-containing molecules. Herein, we report a strategy for synthesizing allyl *gem*-difluorides bearing (*E*)-vinyl boronic esters (Scheme 1c). A newly synthesized 3-boryl-1,1-difluoro allylboronic ester undergoes LiOtBu-mediated deborylative allylation with allyl bromides through two distinct pathways: α-allylation, which produces intermediates that undergo Cope rearrangement,[12] and γ-allylation, which directly affords the same products. Mechanistic investigations demonstrate that the combined effects of the 1,1-difluoro substituents and the boronic ester significantly lower the activation barrier of the rearrangement, enabling efficient and selective access to diverse allyl *gem*-difluorides.
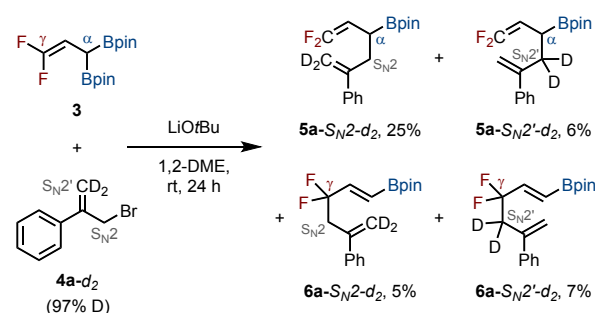
Results and discussion

We first hypothesized that if we could synthesize 3-boryl-1,1-difluoro allylboronic ester, it could serve as a versatile synthon for the synthesis of structurally diverse allyl *gem*-difluorides via
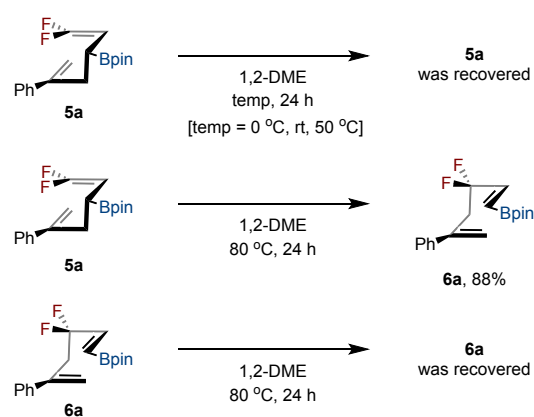
deborylative C–C bond formation with allyl electrophiles. To realize this concept, we first developed a method for preparing the target 3-boryl-1,1-difluoro allylboronic ester. Drawing inspiration from our previous work on palladium-catalyzed cross-coupling of organo(pseudo)halides with diborylmethylzinc halides,[13] we applied related conditions to this system. When 2,2-difluorovinyl *p*-toluenesulfonate (**1**) and diborylmethylzinc halide (**2**) were subjected to Pd(TFA)$_2$ catalysis with RuPhos as the ligand in THF at 80 °C, the desired 3-boryl-1,1-difluoro allylboronic ester (**3**) was obtained in 90% yield on a gram scale (1.5 g, Scheme 2a).

With compound **3** in hand, we next investigated its reactivity in base-promoted deborylative C–C bond-forming reactions[14] with allyl electrophiles (Scheme 2b). As a model study, (3-bromoprop-1-en-2-yl)benzene (**4a**) was reacted with **3** under LiOtBu in 1,2-dimethoxyethane (1,2-DME) at 80 °C. After 1 h, a mixture of the α-addition product **5a** (59%) and the γ-addition product **6a** (25%) was obtained, with **5a** as the major product (entry 1). Extending the reaction time to 12 h decreased the yield of **5a** (26%) while increasing that of **6a** (56%, entry 2). After 24 h, **6a** was formed exclusively in 88% yield (entry 3). Lowering the reaction temperature led to the formation of a mixture of **5a** and **6a**, with **5a** as the major product (entries 4-6).

To confirm whether **6a** arises from the Cope rearrangement of **5a**, we conducted control experiments (Scheme 2c). When pure **5a** was subjected to the reaction conditions at 0-50 °C, no
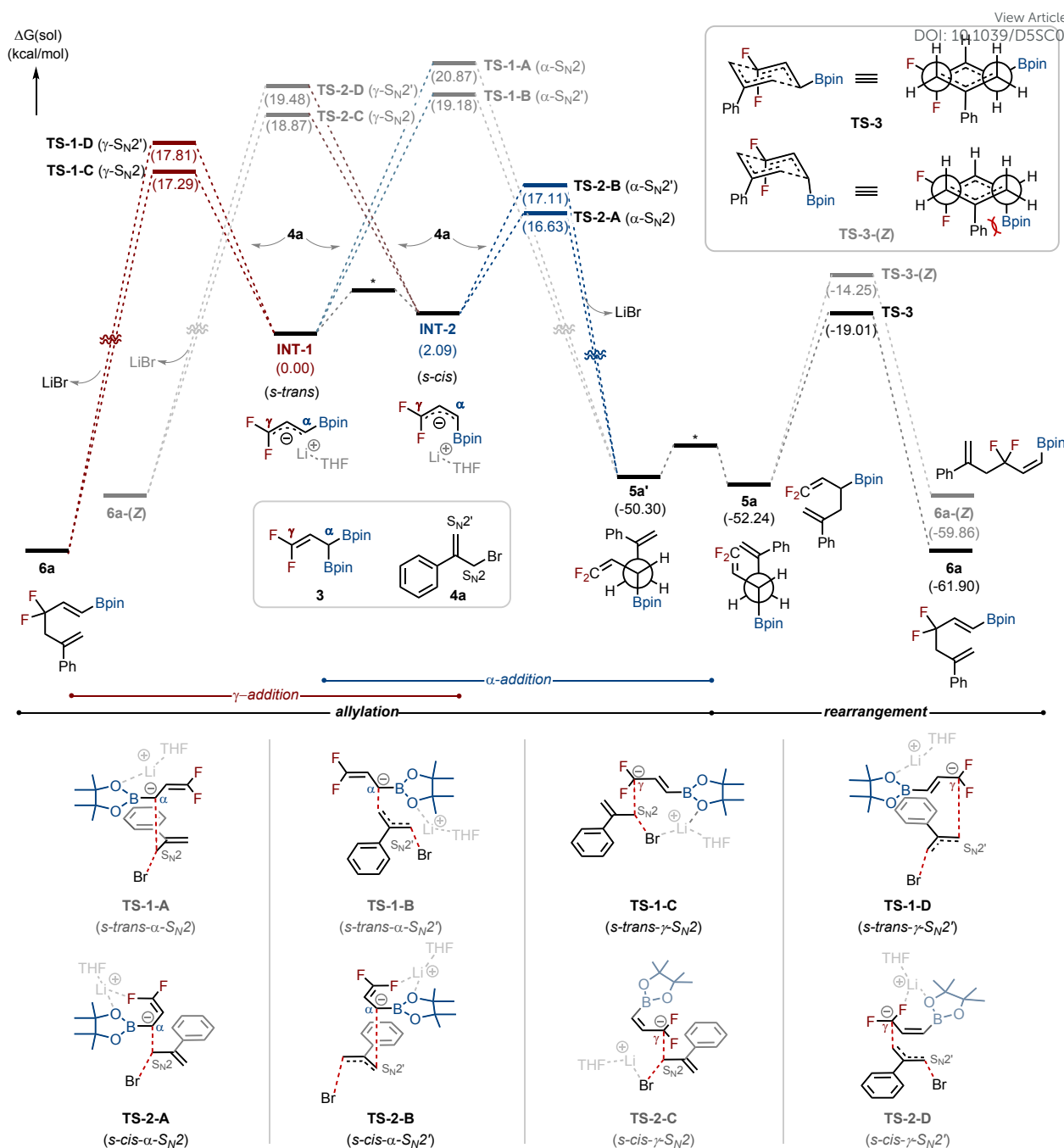
**Scheme 3** Energy profile for the allylation and Cope rearrangement.

conversion occurred. At 80 °C, however, **5a** was quantitatively transformed into **6a**. In contrast, subjecting **6a** to the same conditions resulted in no reversion to **5a**. The optimization studies and control experiments indicated that the LiO*t*Bu-mediated coupling of **3** with **4a** proceeds via two competing pathways: γ-addition, which directly furnishes **6a**, and α-addition, which yields **5a** that undergoes irreversible Cope rearrangement to **6a** at elevated temperature. To further probe the pathway, deuterium-labeling experiments were performed with **3** and deuterium-labeled allyl bromide **4a**-*d₂* at room temperature (Scheme 2d). In this reaction, four distinct

products were obtained, **5a**-S_N2-*d₂* (25%), **5a**-S_N2'-*d₂* (6%), **6a**-S_N2-*d₂* (5%), and **6a**-S_N2'-*d₂* (7%), showing that the reaction can proceed through all four possible pathways: nucleophilic attack from either the α-or γ-position of **3**, occurring via S_N2 or S_N2' displacement on allyl bromide **4a**.
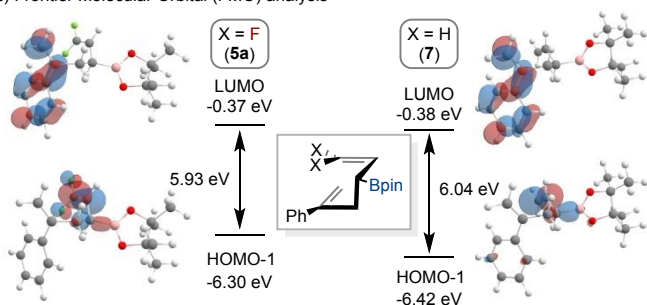
To gain deeper insight into the reaction pathways, we performed density functional theory (DFT) calculations at the SMD (THF) ωB97X-D4/def2-TZVPP//B3LYP/6-31G* level of theory (Scheme 3). THF was chosen as the model solvent, rather than 1,2-DME, to account for possible solvent coordination effects while reducing computational cost and complexity. In
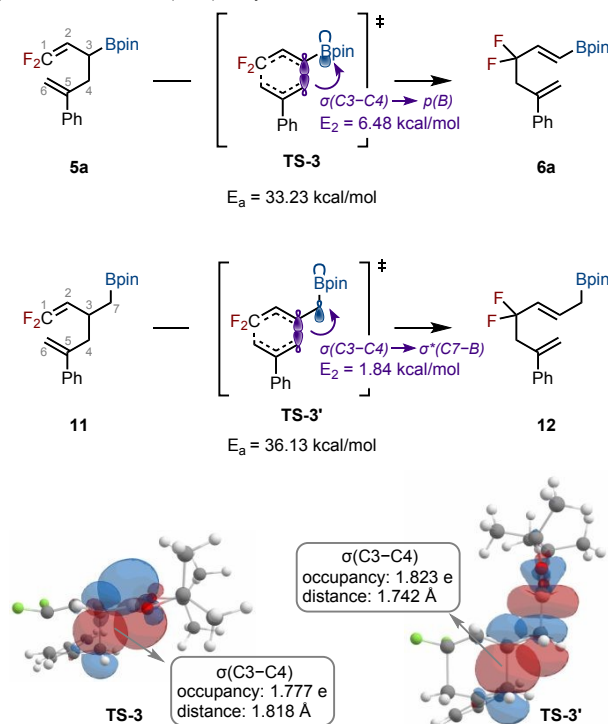
ARTICLE
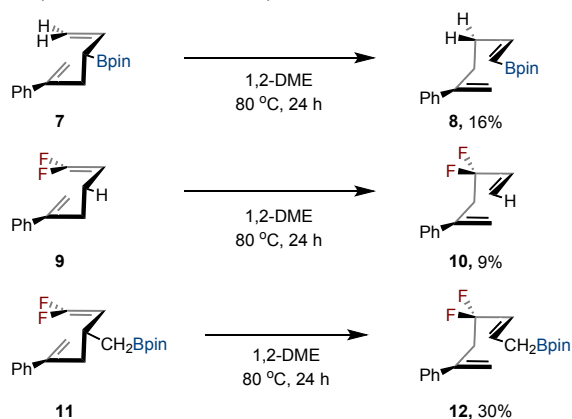
Scheme 4 Control experiments and computational mechanistic studies.

the presence of LiO*t*Bu, 3-boryl-1,1-difluoro allylboronic ester **3** generates boron-ate species that undergoes C–B bond cleavage to form the *s-trans* carbanion **INT-1**, which can isomerize to *s-cis* carbanion **INT-2** (See the Supplementary information for details). Both intermediates are competent for allylation with allyl bromide **4a**, either at the α- or γ-position, and each can proceed via S_N2 or S_N2' displacement, which gives rise to four possible pathways: α-S_N2, α-S_N2', γ-S_N2, and γ-S_N2'. The calculations revealed distinct conformational preferences. Allylation at the α-position of the carbanion (α-S_N2 and α-S_N2') proceeds preferentially through **INT-2**, with lower activation barriers (**TS-2-A**: 16.63 kcal/mol; **TS-2-B**: 17.11 kcal/mol) than through **INT-1** (**TS-1-A**: 20.87 kcal/mol; **TS-1-B**: 19.18 kcal/mol). In contrast, γ-allylation (γ-S_N2, γ-S_N2') is favored via **INT-1** (**TS-1-C**: 17.29 kcal/mol; **TS-1-D**: 17.81 kcal/mol) over **INT-2** (**TS-2-C**: 18.87 kcal/mol; **TS-2-D**: 19.48 kcal/mol). Overall, **TS-2-A** (α-S_N2 from **INT-2**) was identified as the most favorable transition state, followed by **TS-2-B**, **TS-1-C**, and **TS-1-D**. Taken together, these results indicate that all four pathways are energetically accessible, in full agreement with the deuterium-labeling experiments that revealed the participation of each route, and they provide the foundation for analyzing the subsequent Cope rearrangement step. Because allyl bromide **4a** is symmetric, both S_N2 and S_N2' pathways at a given position lead to the same product. The γ-addition pathways directly deliver **6a**, whereas the α-addition pathways first generate conformer **5a'**, which relaxes to **5a** by bond rotation and then undergoes a chair-like Cope rearrangement (**TS-3**) to yield the thermodynamically favored product **6a**. These computational findings align well with the experimental selectivities summarized in Scheme 2b.

We further examined the origin of stereoselectivity in the Cope rearrangement, as only (*E*)-vinylboronic esters were observed. Calculations revealed a substantial energy difference between the competing transition states: **TS-3** leading to the (*E*)-isomer had a lower activation energy (–19.01 kcal/mol), whereas **TS-3-(Z)** was significantly higher (–14.25 kcal/mol). The 4.76 kcal/mol gap arises from steric interactions, as visualized in Newman projections: in **TS-3-(Z)**, severe steric repulsion occurs between the aryl substituent and the Bpin group, whereas **TS-3** allows a more favorable spatial arrangement. As a result, the rearrangement proceeds predominantly via **TS-3**, accounting for the exclusive (*E*)-selectivity observed experimentally.

Next, the potential roles of fluorine and boron substituents in the Cope rearrangement of **5a** to **6a** were examined through a series of control experiments (Scheme 4a). When allyl boronicester **7**, lacking fluorine substituents, was subjected to the standard conditions, the rearranged product **8** was obtained in only 16% yield. In the case of compound **9**, a derivative of **5a** without the Bpin group, product **10** was formed in merely 9% yield, with 91% of the starting material recovered. To further probe the influence of the boron substituent, we tested compound **11**, bearing a CH$_2$Bpin group instead of Bpin, which furnished product **12** in only 30% yield. These results strongly indicate that both the geminal difluoro substituents and the

Journal Name

ARTICLE

Bpin moiety are essential, together exerting a cooperative effect that promotes the Cope rearrangement.

Further computational studies were undertaken to gain a more detailed understanding of the Cope rearrangement. To probe the role of the Bpin group,[15] we compared compounds **5a** and **11**, focusing on their transition states **TS-3** and **TS-3'** (Scheme 4b). The activation barrier for **TS-3** (33.23 kcal/mol) was substantially lower than that for **TS-3'** (36.13 kcal/mol), highlighting the influence of the Bpin substituent. Natural bond orbital (NBO) analysis[16] provided insight into this difference. In **TS-3**, the σ (C3–C4) bond is aligned with the vacant *p* orbital of boron [*p*(B)], enabling efficient σ→*p*(B) electron delocalization and leading to a strong NBO interaction (E_2 = 6.48 kcal/mol). By contrast, in **TS-3'** the σ (C3–C4) bonding orbital is aligned with the σ*(C7–B) antibonding orbital, exhibiting a weaker interaction (E_2 = 1.84 kcal/mol). This enhanced delocalization in **TS-3** reduces the σ (C3–C4) bond occupancy (1.777 e vs 1.823 e in **TS-3'**) and elongates the bond (1.818 Å), thereby weakening the C3–C4 bond and lowering the barrier for rearrangement.

Building upon our investigation of the influence of the boron unit, we next examined the role of fluorine substituents[17] by conducting frontier molecular orbital (FMO) analysis[18] of **5a** and its non-fluorinated analogue **7** (Scheme 4c). For the difluorinated substrate **5a**, the π orbital of the internal C=C bond corresponds to the HOMO-1,[19] while the π* orbital of the terminal C=C bond corresponds to the LUMO. Comparison with **7** (X = H) revealed a reduced [HOMO-1]–[LUMO] gap in **5a**, arising from an elevation of the HOMO-1 energy by 0.12 eV. This electronic perturbation is attributed to the mesomeric electron-donating contribution of the fluorine substituents via *p*-π conjugation[20] (See the Supplementary information for details).

With this mechanistic understanding, we next examined the substrate scope of allyl bromides **4** in the developed allylation/Cope rearrangement sequence (Table 1). A range of C2-aryl-substituted allyl bromides bearing electron-neutral, electron-donating, or electron-withdrawing groups at the *para*-position of the phenyl ring furnished products **6a-6h** in excellent yields. Substituents at the *meta*- and *ortho*-positions of the C2-phenyl group were also tolerated, delivering products **6i-6k**, although **6k** was obtained only in low yield even at elevated temperature. Allyl bromides having 3,5-dimethylphenyl, protected catechol, naphthyl, and benzofuran groups, also underwent the reaction smoothly to give **6l-6o** in low to good yields. Of note, *para*-methoxy- and naphthyl-substituted allyl bromides (**4b** and **4n**) exhibited thermal sensitivity, which was addressed by performing the initial allylation with **3** at 0 °C for 24 h, followed by heating to 80 °C for 12 h. Beyond aryl substitution, allyl bromides bearing aliphatic groups at the C2 position also proved viable, although higher temperatures were required. Substrates with methyl, hexyl, or cyclohexyl groups furnished **6p-6r** in moderate yields. Allyl bromides containing protected amines and *tert*-butyldimethylsilyl (TBS) ethers also participated, affording **6s** and **6t**, respectively. In contrast, cinnamyl bromide underwent only the initial allylation to give 1,1-difluorinated 1,5-hexadiene **5u**, without subsequent Cope rearrangement, even under forcing conditions (150 °C, 24 h). This outcome is likely due to the energetic penalty associated

Table 1 Substrate Scope[a]
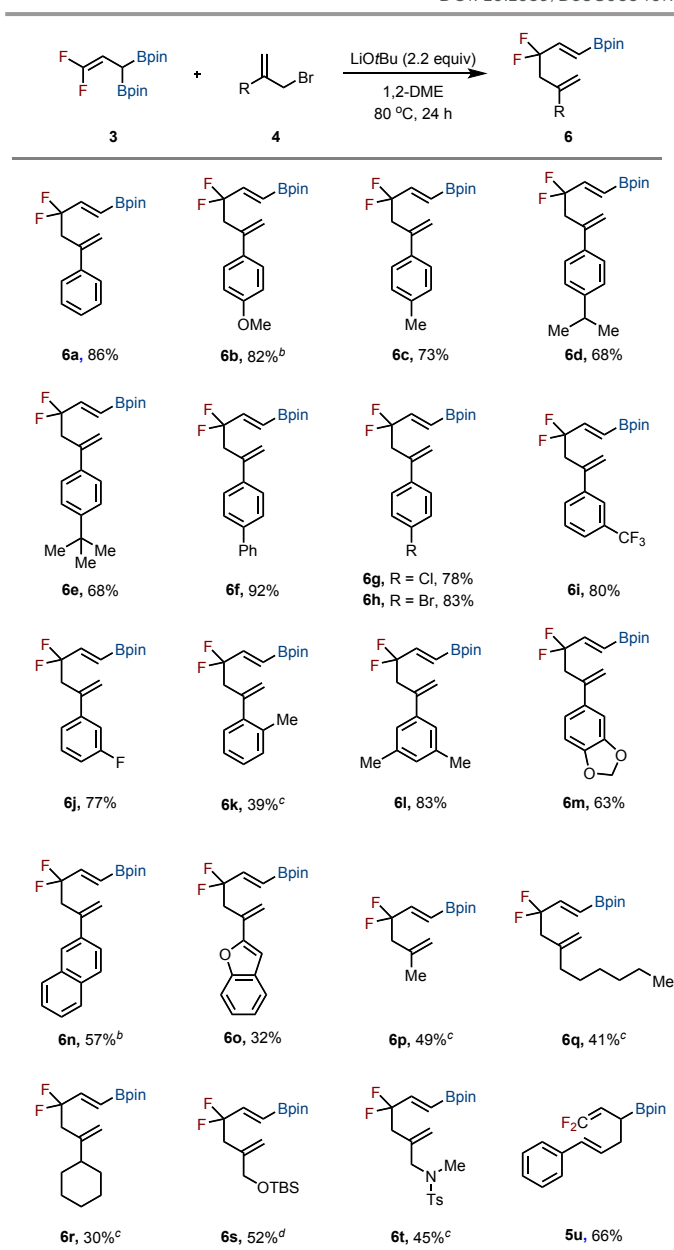
[a]The reaction was performed on 0.1 mmol scale with **4** (0.1 mmol), **3** (0.22 mmol), LiO*t*Bu (0.22 mmol) in 1,2-DME at 80 °C for 24 h. In all cases, isolated yields are indicated. [b]Runs at 0 °C for 24 h, then 80 °C for 12 hr. [c]Runs at 150 °C for 24 hr. [d]Runs at 150 °C for 30 hr.

with disrupting π-conjugation and steric hindrance from the phenyl group.

The obtained allyl *gem*-difluorides bearing (*E*)-vinyl boronic esters serve as valuable precursors for synthesizing diverse *gem*-difluoro-containing molecules. To demonstrate the scalability and practicability of this method, a gram-scale reaction was performed (Scheme 5). Treatment of **4a** (5.0 mmol) with **3** (2.2 equiv) furnished **6a** in 60% yield after extended reaction time. It should be noted that the crude product could be used directly in subsequent transformations without purification. Deuterium incorporation by

protodeboronation of **6a** by treatment with a stoichiometric amount of AgF in
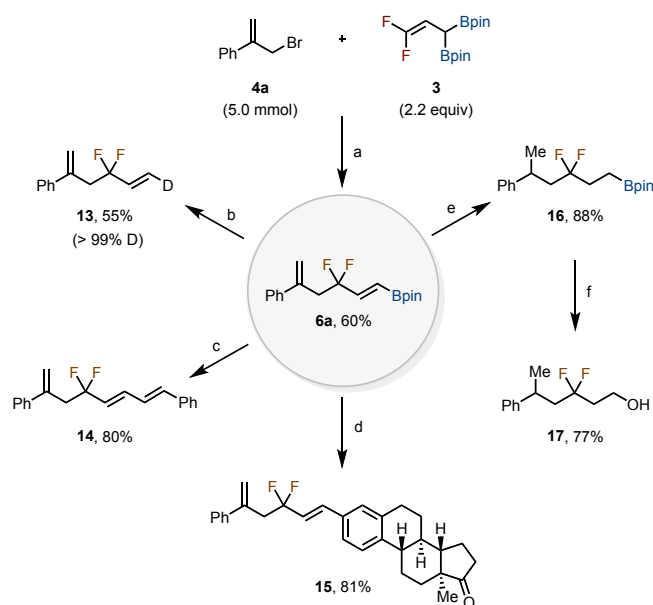
Scheme 5 Synthetic applications. **6a** was used directly without further purification. The yield of **6a** was determined by ^{1}H NMR using CH_2Br_2 as an internal standard. Reaction conditions: (a) LiO*t*Bu, 1,2-DME, 0 °C, 30 h, then 90 °C, 64 h. (b) AgF, THF/D_2O/MeOD, 80 °C, 2 h. (c) *cat.* Pd(PPh$_3$)$_4$, NaOH, β-bromostyrene, toluene/H_2O, 80 °C, 6 h. (d) *cat.* Pd(PPh$_3$)$_4$ Cs$_2$CO$_3$, estrone-derived triflate, toluene/H_2O, 80 °C, 18 h. (e) Pd/C, H_2, MeOH, 60 °C, 3 h. (f) NaOH, H_2O_2, THF, 0 °C to rt, 2 h.

THF/D_2O/MeOD at 80 °C afforded the product **13** in 55% yield with >99% deuterium incorporation.[21] Palladium-catalyzed Suzuki-Miyaura cross-coupling of the vinyl Bpin moiety of **6a** with β-bromostyrene gave the product **14** in 80% yield,[22] while an analogous cross-coupling of **6a** with an estrone-derived triflate afforded **15** in 81% yield.[23] Hydrogenation of the alkenes in **6a** in the presence of 10 mol% Pd/C in MeOH at 60 °C under H_2 atmosphere (1 atm) yielded the corresponding *gem*-difluoroalkyl molecule containing a terminal Bpin group (**16**) in 88% yield.[24] Subsequent oxidation of the Bpin group of **16** produced the corresponding *gem*-difluoroalkyl alcohol **17** in 77% yield.[25]

Conclusions

In summary, we have developed a strategy that enables the synthesis of allyl *gem*-difluorides through a deborylative allylation/Cope rearrangement sequence. The key feature of this approach is the newly designed 3-boryl-1,1-difluoro allylboronic ester, which orchestrates multiple mechanistic pathways yet converges to structurally defined (*E*)-vinylboronic esters. Comprehensive experimental and computational studies establish that the 1,1-difluoro substituents and the boronic ester act in concert to lower the barrier of the rearrangement and dictate stereochemical outcomes. The developed reaction demonstrates broad substrate scope, gram-

scale scalability, and versatile synthetic applications that underscore its value for constructing fluorinated scaffolds.

Author contributions

H. K. and S. C. conceived, designed, and wrote the manuscript. H. K. and S. H. carried out the mechanistic studies. H. K., Y. J., and Y. J. carried out the experiments. S. C. organized the research. All authors discussed the results and commented on the manuscript.

Conflicts of interest

The authors declare no competing interests.

Data availability

The data supporting this article have been included as part of the Supplementary Information.

Acknowledgements

Notes and references

1   (*a*) K. Müller, C. Faeh and F. Diederich, *Science*, 2007, **317**, 1881; (*b*) W. K. Hagmann, *J. Med. Chem.*, 2008, **51**, 4359; (*c*) S. Purser, P. R. Moore, S. Swallow and V. Gouverneur, *Chem. Soc. Rev.*, 2008, **37**, 320; (*d*) J. Wang, M. Sánchez-Roselló, J. L. Aceña, C. del Pozo, A. E. Sorochinsky, S. Fustero, V. A. Soloshonok and H. Liu, *Chem. Rev.*, 2014, **114**, 2432.
2   (*a*) X. Yang, T. Wu, R. J. Phipps and F. D. Toste, *Chem. Rev.*, 2015, **115**, 826; (*b*) C. Ni and J. Hu, *Chem. Soc. Rev.*, 2016, **45**, 5441; (*c*) F. Zhao, W. Zhou and Z. Zuo, *Adv. Synth. Catal.*, 2022, **364**, 234.
3   (*a*) E. P. Gillis, K. J. Eastman, M. D. Hill, D. J. Donnelly and N. A. Meanwell, *J. Med. Chem.*, 2015, **58**, 8315; (*b*) N. A. Meanwell, *J. Med. Chem.*, 2018, **61**, 5822.
4   (*a*) J. B. Y. Wang, N. Serradell, *Drugs Future*, 2006, **31**, 788; (*b*) Y. N. Lamb, *Drugs*, 2017, **77**, 1797.
5   For selected examples of the application of allyl *gem*-difluorides, see: (*a*) T. Narumi, K. Tomita, E. Inokuchi, K. Kobayashi, S. Oishi, H. Ohno and N. Fujii, *Org. Lett.*, 2007, **9**, 3465; (*b*) Y. Yamaki, A. Shigenaga, K. Tomita, T. Narumi, N. Fujii and A. Otaka, *J. Org. Chem.*, 2009, **74**, 3272; (*c*) M. Bergeron, T. Johnson and J.-F. Paquin, *Angew. Chem. Int. Ed.*, 2011, **50**, 11112; (*d*) H. Yanai, H. Okada, A. Sato, M. Okada and T. Taguchi, *Tetrahedron Lett.*, 2011, **52**, 2997; (*e*) T. A. Unzner and T. Magauer, *Tetrahedron Lett.*, 2015, **56**, 877; (*f*) L.-n. Tang, G.-y. Liu, J.-h. Li and M. Chen, *Org. Lett.*, 2023, **25**, 9064; (*g*) G.-y. Liu,

Chemical Science Accepted Manuscript

L.-n. Tang, J.-h. Li, S. Yang and M. Chen, *Chem. Commun.*, 2024, **60**, 4471.

6   D. Tomon and S. Arimitsu, *Eur. J. Org. Chem.*, 2025, **28**, e202401162.

7   For selected examples of the synthesis of allyl *gem*-difluorides, see: (*a*) X. Yue, X. Zhang and F.-L. Qing, *Org. Lett.*, 2009, **11**, 73; (*b*) G. K. S. Prakash, S. K. Ganesh, J.-P. Jones, A. Kulkarni, K. Masood, J. K. Swabeck and G. A. Olah, *Angew. Chem. Int. Ed.*, 2012, **51**, 12090; (*c*) Q.-Q. Min, Z. Yin, Z. Feng, W.-H. Guo and X. Zhang, *J. Am. Chem. Soc.*, 2014, **136**, 1230; (*d*) M. Ke, Q. Feng, K. Yang and Q. Song, *Org. Chem. Front.*, 2016, **3**, 150; (*e*) C.-Q. Wang, Y. Zhang and C. Feng, *Angew. Chem. Int. Ed.*, 2017, **56**, 14918; (*f*) Z. Zhao, L. Racicot and G. K. Murphy, *Angew. Chem. Int. Ed.*, 2017, **56**, 11620; (*g*) G. Wu and A. Jacobi von Wangelin, *Chem. Sci.*, 2018, **9**, 1795; (*h*) W.-H. Guo, H.-Y. Zhao, Z.-J. Luo, S. Zhang and X. Zhang, *ACS Catal.*, 2019, **9**, 38; (*i*) L. Tang, Z.-Y. Liu, W. She and C. Feng, *Chem. Sci.*, 2019, **10**, 8701; (*j*) L. Liao, R. An, H. Li, Y. Xu, J.-J. Wu and X. Zhao, *Angew. Chem. Int. Ed.*, 2020, **59**, 11010; (*k*) F. Ye, Y. Ge, A. Spannenberg, H. Neumann, L.-W. Xu and M. Beller, *Nat. Commun.*, 2021, **12**, 3257; (*l*) C. Zhu, M.-M. Sun, K. Chen, H. Liu and C. Feng, *Angew. Chem. Int. Ed.*, 2021, **60**, 20237; (*m*) X.-T. Feng, J.-X. Ren, X. Gao, Q.-Q. Min and X. Zhang, *Angew. Chem. Int. Ed.*, 2022, **61**, e202210103; (*n*) T. Dong, Y. Ye, Y. Wang, K. P. S. Cheung and G. C. Tsui, *Chem. Asian J.*, 2023, **18**, e202300655; (*o*) Z. Fu and G. C. Tsui, *Org. Chem. Front.*, 2024, **11**, 4697; (*p*) M. Zhou, J.-X. Ren, X.-T. Feng, H.-Y. Zhao, X.-P. Fu, Q.-Q. Min and X. Zhang, *Chem. Sci.*, 2024, **15**, 2937; (*q*) Z.-X. Wang, N. A. Heckmann, C. G. Daniliuc and R. Gilmour, *Angew. Chem. Int. Ed.*, 2025, e202518520.

8   (*a*) Y.-G. Lou, A.-J. Wang, L. Zhao, L.-F. He, X.-F. Li, C.-Y. He and X. Zhang, *Chem. Commun.*, 2019, **55**, 3705; (*b*) S. Sakamoto, T. W. Butcher, J. L. Yang and J. F. Hartwig, *Angew. Chem. Int. Ed.*, 2021, **60**, 25746.

9   For selected examples using 1,1-difluoro allylmetalloids, see: (*a*) G.-q. Shi and X.-h. Huang, *Tetrahedron Lett.*, 1996, **37**, 5401; (*b*) F. Tellier, M. Baudry and R. Sauvêtre, *Tetrahedron Lett.*, 1997, **38**, 5989; (*c*) P. Veeraraghavan Ramachandran and A. Chatterjee, *Org. Lett.*, 2008, **10**, 1195; (*d*) P. V. Ramachandran, A. Tafelska-Kaczmarek and A. Chatterjee, *J. Org. Chem.*, 2012, **77**, 9329; (*e*) Y. Liu, Y. Zhou, Y. Zhao and J. Qu, *Org. Lett.*, 2017, **19**, 946; (*f*) R. Kojima, S. Akiyama and H. Ito, *Angew. Chem. Int. Ed.*, 2018, **57**, 7196; (*g*) X. Yang, Z.-H. Cao, Y. Zhou, F. Cheng, Z.-W. Lin, Z. Ou, Y. Yuan and Y.-Y. Huang, *Org. Lett.*, 2018, **20**, 2585; (*h*) P. H. S. Paioti, J. del Pozo, M. S. Mikus, J. Lee, M. J. Koh, F. Romiti, S. Torker and A. H. Hoveyda, *J. Am. Chem. Soc.*, 2019, **141**, 19917; (*i*) G. Chen, L. Wang, X. Liu and P. Liu, *Adv. Synth. Catal.*, 2020, **362**, 2990; (*j*) N. A. Phillips, G. J. Coates, A. J. P. White and M. R. Crimmin, *Chem. - Eur. J.*, 2020, **26**, 5365; (*k*) J. Qi, F.-L. Zhang, J.-K. Jin, Q. Zhao, B. Li, L.-X. Liu and Y.-F. Wang, *Angew. Chem. Int. Ed.*, 2020, **59**, 12876; (*l*) C. Luo, Y. Zhou, H. Chen, T. Wang, Z.-B. Zhang, P. Han and L.-H. Jing, *Org. Lett.*, 2022, **24**, 4286; (*m*) N. Oyama, S. Akiyama, K. Kubota, T. Imamoto and H. Ito, *Eur. J. Org. Chem.*, 2022, **2022**, e202200664.

10   (*a*) W. Jo, J. H. Lee and S. H. Cho, *Chem. Commun.*, 2021, **57**, 4346; (*b*) Y. Lee, S. Han and S. H. Cho, *Acc. Chem. Res.*, 2021, **54**, 3917.

11   (*a*) A. B. Cuenca, R. Shishido, H. Ito and E. Fernández, *Chem. Soc. Rev.*, 2017, **46**, 415; (*b*) N. Miralles, R. J. Maza and E. Fernández, *Adv. Synth. Catal.*, 2018, **360**, 1306; (*c*) R. Nallagonda, K. Padala and A. Masarwa, *Org. Biomol. Chem.*, 2018, **16**, 1050; (*d*) C. Zhang, W. Hu and J. P. Morken, *ACS Catal.*, 2021, **11**, 10660; (*e*) X. Li, J. Chen and Q. Song, *Chem. Commun.*, 2024, **60**, 2462.

12   (*a*) S. T. Purrington and S. C. Weeks, *J. Fluor. Chem.*, 1992, **56**, 165; (*b*) E. A. Ilardi, C. E. Stivala and A. Zakarian, *Chem. Soc. Rev.*, 2009, **38**, 3133; (*c*) H. M. L. Davies and Y. Lian, *Acc. Chem. Res.*, 2012, **45**, 923; (*d*) Y. Liu, X. Liu and X. Feng, *Chem. Sci.*, 2022, **13**, 12290.

13   H. Lee, Y. Lee and S. H. Cho, *Org. Lett.*, 2019, **21**, 5912.

14   (*a*) J. R. Coombs, L. Zhang and J. P. Morken, *J. Am. Chem. Soc.*, 2014, **136**, 16140; (*b*) K. Hong, X. Liu and J. P. Morken, *J. Am. Chem. Soc.*, 2014, **136**, 10581; (*c*) W. Sun, L. Wang, Y. Hu, X. Wu, C. Xia and C. Liu, *Nat. Commun.*, 2020, **11**, 3113.

15   For selected examples of pericyclic reactions with boron compounds, see: (*a*) X. Gao and D. G. Hall, *J. Am. Chem. Soc.*, 2003, **125**, 9308; (*b*) J. Pietruszka and N. Schöne, *Angew. Chem. Int. Ed.*, 2003, **42**, 5638; (*c*) M. Murakami, S. Ashida and T. Matsuda, *J. Am. Chem. Soc.*, 2004, **126**, 10838; (*d*) C. Tillin, R. Bigler, R. Calo-Lapido, B. S. L. Collins, A. Noble and V. K. Aggarwal, *Synlett*, 2019, **30**, 449; (*e*) K. Kanti Das, P. Kumar, D. Ghorai, B. Mondal and S. Panda, *Asian J. Org. Chem.*, 2022, **11**, e202100092; (*f*) Y. Liu, D. Ni and M. K. Brown, *J. Am. Chem. Soc.*, 2022, **144**, 18790; (*g*) J. M. Posz, N. Sharma, P. A. Royalty, Y. Liu, C. Salome, T. C. Fessard and M. K. Brown, *J. Am. Chem. Soc.*, 2024, **146**, 10142; (*h*) S. Adak, P. S. Hazra, C. B. Fox and M. K. Brown, *Angew. Chem. Int. Ed.*, 2025, **64**, e202416215; (*i*) A. Messara, B. Kweon, F. Woge, C. G. Daniliuc, C. Mück-Lichtenfeld and R. Gilmour, *J. Am. Chem. Soc.*, 2025, **147**, 36677; (*j*) J. Taguchi, Y. Ohata, H. Akimoto, H. Tabuchi, K. Igawa, K. Tomooka, T. Niwa and T. Hosoya, *Org. Lett.*, 2025, **27**, 4428.

16   D. V. Vidhani, M. E. Krafft and I. V. Alabugin, *J. Am. Chem. Soc.*, 2016, **138**, 2769.

17   (*a*) W. R. Dolbier, K. S. Medinger, A. Greenberg and J. F. Liebman, *Tetrahedron*, 1982, **38**, 2415; (*b*) K. A. Black, S. Wilsey and K. N. Houk, *J. Am. Chem. Soc.*, 2003, **125**, 6715.

18   S. Wang, H. Wu, X. Tang and G. Huang, *Org. Chem. Front.*, 2024, **11**, 2870.

19   L.-G. Zhuo, W. Liao and Z.-X. Yu, *Asian J. Org. Chem.*, 2012, **1**, 336.

20   For selected examples of the mesomeric effect of fluorine, see: (*a*) W. A. Sheppard, *J. Am. Chem. Soc.*, 1965, **87**, 2410; (*b*) M. Ohashi, K. Ando, S. Murakami, K. Michigami and S. Ogoshi, *J. Am. Chem. Soc.*, 2023, **145**, 23098.

21   Y. Jung and S. H. Cho, *Synlett*, 2023, **34**, 2165.

22   S. Wang, J. Zhang, L. Kong, Z. Tan, Y. Bai and G. Zhu, *Org. Lett.*, 2018, **20**, 5631.

23   W.-H. Guo, H.-Y. Zhao, Z.-J. Luo, S. Zhang and X. Zhang, *ACS Catal.*, 2019, **9**, 38.

24   B. Zhang and X. Zhang, *Chem. Commun.*, 2016, **52**, 1238.

25   Y. Fan, Z. Huang, Y. Lu, S. Zhu and L. Chu, *Angew. Chem. Int. Ed.*, 2024, **63**, e202315974.

View Article Online
DOI: 10.1039/D5SC08976K

Data availability

The data that support the findings of this study are available in the supplementary material of this article.